# Amyloid- peptide-specific DARPins as a novel class of potential therapeutics for Alzheimer disease

Hanenberg, Michael ; McAfoose, Jordan ; Kulic, Luka ; Welt, Tobias ; Wirth, Fabian ; Parizek, Petra ; Strobel, Lisa ; Cattepoel, Susann ; Späni, Claudia ; Derungs, Rebecca ; Maier, Marcel ; Plückthun, Andreas ; Nitsch, Roger M

Abstract: Passive immunization with anti-amyloid- peptide (A ) antibodies is effective in animal models of Alzheimer disease. With the advent of efficient in vitro selection technologies, the novel class of designed ankyrin repeat proteins (DARPins) presents an attractive alternative to the immunoglobulin scaffold. DARPins are small and highly stable proteins with a compact modular architecture ideal for high affinity protein-protein interactions. In this report, we describe the selection, binding profile, and epitope analysis of A -specific DARPins. We further showed their ability to delay A aggregation and prevent A -mediated neurotoxicity in vitro. To demonstrate their therapeutic potential in vivo, mono- and trivalent A -specific DARPins (D23 and 3×D23) were infused intracerebroventricularly into the brains of 11-month-old Tg2576 mice over 4 weeks. Both D23 and 3×D23 treatments were shown to result in improved cognitive performance and reduced soluble A levels. These findings demonstrate the therapeutic potential of A -specific DARPins for the treatment of Alzheimer disease.

DOI: https://doi.org/10.1074/jbc.M114.564013

JBC Papers in Press. Published on August 12, 2014 as Manuscript M114.564013
The latest version is at http://www.jbc.org/cgi/doi/10.1074/jbc.M114.564013


# Aβ-specific DARPins as a novel class of potential therapeutics for Alzheimer's disease

Michael Hanenberg[1], Jordan McAfoose[1], Luka Kulic[1,2,3], Tobias Welt[1], Fabian Wirth[1], Petra Parizek[4], Lisa Strobel[1], Susann Cattepoel[1], Claudia Späni[1], Rebecca Derungs[1], Marcel Maier[5], Andreas Plückthun[4] & Roger M. Nitsch[1]

[1] Division of Psychiatry Research, University of Zurich, Wagistrasse 12, 8952 Schlieren, Switzerland

[2] Department of Neurology, University Hospital Zurich, University of Zurich, Frauenklinikstrasse 26, 8091 Zurich, Switzerland

[3] Zurich Center for Integrative Human Physiology (ZIHP), University of Zurich, Winterthurerstrasse 190, 8057 Zurich, Switzerland

[4] Institute of Biochemistry, University of Zurich, Winterthurerstrasse 190, 8057 Zurich, Switzerland

[5] Neurimmune Holding AG, Wagistrasse 13, 8952 Schlieren, Switzerland

## Conflict of interest

M. Hanenberg, J. McAfoose, Luka Kulic, T. Welt, C. Späni, F. Wirth, R. Derungs and R. M. Nitsch have no competing interests to declare. S. Cattepoel is now an employee of CSL Behring AG, but declares no competing interests. M. Maier is now an employee of Neurimmune Holding AG, but declares no competing interests. A. Plückthun is a shareholder of Molecular Partners, commercializing the DARPin technology.

Address correspondence to: Roger M. Nitsch, Division of Psychiatry Research, University of Zurich, Wagistrasse 12, 8952 Schlieren, Switzerland, phone +41 44 634 88 71, fax +41 44 634 88 79, e-mail: nitsch@bli.uzh.ch

**Capsule**

**Background:** The amyloid-beta peptide (Aβ) is crucially involved in the onset and progression of Alzheimer's disease (AD).

**Results:** A designed ankyrin repeat protein (DARPin) was selected to bind and neutralize Aβ.

**Conclusion**: DARPins can prevent amyloid formation and associated neurotoxic effects of Aβ.

**Significance:** DARPins provide a therapeutic potential in the treatment of AD.

**Abstract**

Passive immunization with anti-Aβ antibodies is effective in animal models of Alzheimer's disease (AD). With the advent of efficient *in vitro* selection technologies, the novel class of designed ankyrin repeat proteins (DARPins) presents an attractive alternative to the immunoglobulin scaffold. DARPins are small and highly stable proteins with a compact modular architecture ideal for high-affinity protein-protein interactions. In this report we describe the selection, binding profile and epitope analysis of Aβ-specific DARPins. We further showed their ability to delay Aβ aggregation and prevent Aβ-mediated neurotoxicity *in vitro*. To demonstrate their therapeutic potential *in vivo*, mono- and trivalent Aβ-specific DARPins (D23 and 3xD23) were infused intracerebroventricularly into brains of 11 months old Tg2576 mice over four weeks. Both D23 and 3xD23 treatments were shown to result in improved cognitive performance and reduced soluble Aβ levels. These findings demonstrate the therapeutic potential of Aβ-specific DARPins for the treatment of AD.

**Introduction**

The amyloid-β peptide (Aβ) is considered a central component in the onset and progression of Alzheimer's disease (AD)(1). Three major pathways have been identified as potential therapeutic channels to alleviate the clinical progression and cognitive loss: (i) the inhibition of Aβ production from amyloid precursor protein (APP), (ii) interference with the formation of toxic aggregation intermediates and (iii) the accelerated elimination of Aβ from the brain into the periphery(2, 3).

From a clinical point of view, these concepts strongly support the use of therapeutic strategies with proteins that can specifically bind, neutralize, and prevent the aggregation and propagation of misfolded proteins throughout the brain.

Based on the effective clearance of β-amyloid from the brains of mouse models of brain amyloidosis upon repeated Aβ immunization(4, 5), numerous immunotherapy clinical trials in humans have subsequently been initiated(6–8). To-date, more than one dozen anti-amyloid immunotherapy clinical trials, testing both passive immunotherapy and active vaccination strategies, are currently underway for the treatment of AD(9).

Designed ankyrin repeat proteins (DARPins) can be effectively selected *in vitro* for binding to a broad variety of target proteins with high specificity and affinity, and they have been shown to provide new therapeutic avenues(10). DARPins are built from several ankyrin repeat modules that are tightly packed and capped by terminating repeats that shield the hydrophobic core, resulting in high stability and solubility with a low aggregation tendency(11, 12). Additionally, the absence of redox-sensitive disulfide bonds has enabled DARPins to be used for both intracellular and extracellular applications(13, 14) and, combined with the lack of endogenous receptors, allows an improved fine-tuning of tissue distribution and clearance(15) as compared to conventional immunoglobulin-based (IgG) scaffolds. At one-tenth the molecular weight of IgGs, DARPins might cross the blood brain barrier (BBB) more efficiently than antibodies upon peripheral administration(16, 17). Unlike IgG-Aβ complexes(18), DARPins bound to Aβ will probably be removed quickly and efficiently from the body, making them ideal amyloid-lowering therapeutics with a low risk for immunogenicity and production of neutralizing antibodies following repeated administration(19).

Here we describe the selection of a novel class of potential Aβ-specific therapeutics based on the ankyrin fold, their affinity determination as well as their ability to prevent

Aβ aggregation, reduce Aβ-mediated neurotoxicity in a cell-culture model and show its therapeutic potential in APP transgenic mice (Tg2576) *in vivo*, an animal model of Alzheimer's disease.

## Experimental procedures

**Preparation of the amyloid-β peptides.** Recombinant Aβ1–42 peptide was purchased as hexafluoro-isopropanol (HFIP) film from rPeptide (Bogart, USA). All biotinylated variants (Aβ1–28, Aβ1–40 and Aβ1–42) were obtained from Anaspec (Fremont, USA) and processed as previously described(20).

**Ribosome display selection of DARPins.** The enrichment of anti-Aβ DARPins was performed using previously described N2C and N3C DARPin libraries(12). Ribosome display selections using decreasing concentrations of biotinylated Aβ1–28 (400 nM to 100 nM) as target peptide were performed in analogy to previous reports(21). The library was subjected to a total of four selection cycles, the first of which was performed on biotinylated peptide bound to a neutravidin-coated microtiter plate and the three subsequent rounds were carried out in solution using streptavidin-coated magnetic particles for pull-down of the ternary DARPin-ribosome-mRNA complexes.

**Screening and titration ELISA.** DARPin expression and cell lysis were performed as described previously(22). For the analysis of individual DARPin clones microtiter plates (Corning, Amsterdam, The Netherlands) were coated with 66 nM neutravidin followed by immobilization of 250 nM of the target peptides for 1 h at 4ºC. Bound DARPins were detected via an anti-RGS-$His_6$ antibody (Qiagen, dilution 1:1000) followed by an anti-mouse-HRP conjugate (GE Healthcare, dilution 1:2000). The assay was quantified colorimetrically (tetramethylbenzidine in 30 mM citric acid (1:20)) and stopped with 1 M $H_2SO_4$. The absorbance at 450 nm was recorded against a reference wavelength of 690 nm with a standard ELISA reader Sunrise™ (Tecan, Männedorf, Switzerland). The data were fitted to a sigmoid dose-response equation using Graph Pad Prism 5 (GraphPad Software, USA) to calculate the concentration of half-maximal binding ($EC_{50}$).

**Competition ELISA.** Competition studies were performed using a constant concentration of 10 nM DARPin with increasing quantities of soluble Aβ1–42 (0 to 5000 nM in $TBS_{150}$ for 1 h at 4ºC). Target peptide was immobilized at 250 nM. Signal detection was performed as described for titration ELISA.

**Epitope mapping by monoclonal antibodies.** Aβ1–42 at 200 nM was immobilized onto a DARPin D23-coated microtiter plate and probed with 1 ng $\mu L^{-1}$ of the monoclonal antibodies 6E10, 4G8 (Covance, Basel, Switzerland) and 22C4 (in-house). Bound antibodies were detected as described for titration ELISA.

**Epitope mapping by peptide competition**. Aβ1-28-biotin (250 nM solution) was surface-immobilized on a neutravidin layer of a microtiter plate. DARPin D23 at 50 nM was pre-incubated with a 50-fold molar excess of the peptide fragments Aβ(-4-6), Aβ (–3–7), Aβ(–2–8), Aβ(–1–9), Aβ(1–8), Aβ(2–11), Aβ(3–12), Aβ(4–13), Aβ(5–14), Aβ(6–15) (peptides&elephants, Potsdam, Germany), Aβ(1–11), Aβ(1–16), Aβ(12–28), Aβ(29–40), Aβ(31–35), Aβ(33–42), Aβ(1–28), Aβ(1–38) (Bachem, Bubendorf, Switzerland) and scrambled Aβ1–42 (from N- to C-terminus: AIAEGDSHVLKEGAYMEIFDVQGHVFGG KIFRVVDLGSHNVA) (rPeptide, Bogart, USA). The fraction of surface-bound D23 was detected as described for titration ELISA.

**Aβ aggregation assays.** The inhibitory effect of equimolar concentrations of D23 on Aβ1-42 aggregation (both at 5 μM) was assessed in real time by thioflavine T (ThT) fluorescence as described previously(20). The concentration of the Aβ stock solutions were determined spectrophotometrically ($\varepsilon$ = 1730 $M^{-1}$ $cm^{-1}$) and, for reasons of reproducibility, used within 24 hours of preparation(23). The elongation rates were mathematically deduced via linear regression from the aggregation curves using signals from 20 to 80% of the steady state for all three experimental conditions.

**Neurotoxicity assays.** The neuroprotective effect of D23 on Aβ-mediated neurotoxicity (both at 5 μM) was investigated in a cell culture model of primary cortical neurons from rat embryos (day E18) and performed identically to previously published protocols(20). Three wells per treatment were measured and the assay repeated two more times. Data are given as means ± SEM.

**Cloning strategy for multivalent DARPins.** The coding sequence of D23 was excised from the expression plasmid pQE30 (Qiagen, Hildesheim, Germany) using the restriction enzymes BamHI and HindIII (New England Biolabs, Ipswich, USA) and subsequently inserted into the recipient plasmid (pQI-bi-1_1) via a BamHI/HindIII (cassette 1) and BglII and BsaI (cassette 2) restriction digestion. Trivalent D23 was constructed from bivalent D23 via PCR using the primers MVD3_forw (5'-AAAGAGGAGAAATTAACTATGAGAGGATC-3') and QiBi_MVD_rev (5'-AAGGATAGGTCTCAAGCTAGAGAGTCATTACCCCAGGCGTTTAAGG-3'), the resulting amplificate being digested with BamHI / BsaI and inserted into the pQI-bi-1_1 recipient vector via its restriction sites for BglII and BsaI. The vector had previously been modified to already contain a DARPin in the 5'-expression cassette. DARPins were genetically engineered as head-to-tail fusions and expressed in a single open reading frame (ORF) as previously described(15).

**Surface plasmon resonance**. SPR was recorded with a Biacore T100 instrument (GE Healthcare) similarly to previous descriptions using a streptavidin-coated sensor chip and Aβ1-42-biotin as immobilized target(12). Association and dissociation events were measured at a constant flow rate of 30 μL $min^{-1}$ with analyte concentrations doubling from 0.5 nM to 512 nM. Kinetic data were globally fitted to a 1:1 binding model (D23) or a bivalent binding model (3xD23) as part of the BIAevaluation software 2.0.3 (GE Healthcare), but the complicated kinetics of 3xD23 preclude a numeric evaluation.

**Animals.** This study used Tg2576 transgenic mice expressing human APP carrying the Swedish mutation K670N/M671L(24). A 12 hour light–dark cycle was maintained in the housing room and, except for the time of testing, water and food was provided *ad libitum*.

**Cognitive-behavioral testing.** At the time of testing, mice were weighed and examined for general health indicators to ensure that the mice were physically able to conduct the cognitive-behavioral test and to rule out any adverse side effects due to the surgical procedure or DARPin therapy (cf. Supplementary Material). Spatial working memory was assessed in mice using the Y-maze (Y-shaped plastic maze, with 40 cm x 20 cm x 10 cm arm sizes). During a 5 min trial the sequence of arm entries was recorded using the ANY-maze Video Tracking System (Stoelting Co., USA). The percent alternation was calculated as the ratio of actual to possible alternations (defined as the total number of arm entries –2) x 100%.

**DARPin intracerebroventricular (icv) administration via surgical implantation of Alzet® osmotic minipumps.** Twelve-month-old Tg2576 mice were deeply anaesthetized, a small midline incision was made to expose the skull, and a subcutaneous pocket was prepared in the midscapular area of the back of the mice so that a sterile Alzet® minipump (model 2004) filled with DARPin solution or vehicle could be inserted. Subsequently, an Alzet Brain infusion kit 3 cannula was lowered into the left lateral ventricle (coordinates according to bregma; AP,–0.2 mm; ML, 0.9 mm; and DV, 2.5 mm) and two small screws were placed within the skull and dental cement applied to firmly attach to the skull. Groups of 19–23 mice received icv-infusion over 28 days (equimolar concentration of 50 μM) of either D23, 3xD23, E2_5 or PBS control.

**Biochemical and histochemical analyses.** Brains from treated mice were obtained as described previously(25). The right hemibrain was homogenized using a sequential extraction protocol using a glass-Teflon homogenizer (20 strokes, 315 rpm) in RIPA buffer containing complete protease inhibitor tablets (Sigma-Aldrich, Switzerland). The brain extract was ultra-centrifuged (100,000 x g at 4ºC for 1

hour), supernatant extracted and stored at –80°C for later biochemical analysis. The remaining pellet was frozen on dry ice, resuspended in 70% formic acid, sonicated for 30 s at 30% power and ultra-centrifuged (30 min). The supernatant was extracted, lyophilized, reconstituted in RIPA buffer and stored at –80°C for later analysis.

**Beta-amyloid analysis**. Aβ fragments were measured in plasma and brain homogenates using a MSD 3plex multi-SPOT Abeta human kit (MesoScale Discovery, USA), based on electrochemiluminescence detection, with capture antibodies specific for Aβx-38, Aβx-40 and Aβx-42, in accordance to the manufacturer's instructions. The MSD SECTOR Imager 6000 reader was used for analysis and the MSD DISCOVERY WORKBENCH software (Version 3.0.17) with the Data Analysis Toolbox was used to calculate sample concentrations by comparing them against a standard curve (five-parameter logistic curve).

**Histochemistry.** Thioflavin S staining was done according to a previously published protocol(25). All chemicals were obtained from Sigma (St. Louis, MO). Antibody 4G8 (Covance, Basel, Switzerland) was used at 1 ng $\mu L^{-1}$ to detect amyloid deposits.
The effect of Aβ addition on neuronal morphology was observed in a cell culture model of primary cortical neurons from rat embryos (day E18) and performed as previously described (20). Shortly, cells were washed in PBS, fixated by 4% paraformaldehyde (in PBS) for 15 min and subsequently washed by TBS + 0.05% Triton X-100. Cells were blocked with a mixture of 5% goat- and 5% horse serum (in TBS + 0.05% Triton X-100) for 1h at 4°C. Aβ deposits were visualized by a polyclonal anti-Aβ antibody (Zymed Lab., USA) at 1:500, neurons were stained by an anti-MAP2 antibody (Sigma, St. Gallen, Switzerland) at 1:1000, followed by secondary Cy2-/Cy3-antibodies.

**Statistical analysis.** Data analysis was performed using GraphPad Prism 4.03 software. Tests for normal distribution were performed before statistical testing, according to the results of the Shapiro-Wilk and the Kolmogorov-Smirnov Test for normality. Either Student's t Test or Mann-Whitney U Test for 2 sample groups or ANOVA for multiple comparisons was performed (followed by post-hoc Tukey's or Mann-Whitney U test). A p-value $< 0.05$ was considered statistically significant. Error bars are SEM if not indicated differently.

**Approval Animal Studies.** All animal experiments were approved by the veterinary office of the Cantonal Health Department Zurich.

## Results

### DARPin D23 specifically binds to soluble monomeric Aβ.

Ribosome display was used to enrich specific DARPins against the Aβ peptide. Libraries in the N2C and N3C format (with 2 or 3 randomized repeats between the N- and C-capping repeats) were subjected to surface-immobilized C-terminally biotinylated Aβ1–28. This truncated Aβ variant was chosen over Aβ1–42 for its reduced propensity to form aggregates. In every round, the selection pressure was increased through a decrease in the amount of target peptide, increased washing stringency and a reduced number of PCR cycles to re-amplify the selected sub-pool. From cycle 2 onwards, selection was performed in solution to drive the selection of DARPins towards recognizing soluble Aβ species (**Figure 1a**). After four cycles, a screening ELISA revealed 30 out of 96 clones as specific for Aβ1–28 (31%) with negligible reactivity to control proteins. These controls comprised neutravidin, bovine serum albumin (BSA) and directly (=hydrophobically) coated Aβ1-42. All specific binders came from the N2C library. DNA sequence analysis of twenty randomly selected Aβ binders confirmed differences mainly in the variable interaction residues and with lower frequency also in the N-terminal cap. Due to best performance in a series of binding experiments, the DARPin termed D23 was selected as a lead candidate for further characterization. A titration ELISA (**Figure 1b**) demonstrated that the selected clone also recognized the pathologically relevant variant Aβ1–42 with a similar $EC_{50}$ (17 nM for Aβ1–28 and 31 nM for Aβ1–42). The binding of DARPin D23 to surface-immobilized Aβ was specifically competed using a molar excess of soluble Aβ1–42 with a 50% drop in binding signal at a competitor concentration of < 50 nM, indicating a low nanomolar affinity of D23 for soluble Aβ1–42 (**Figure 1c**).

### D23 binds a conformational Aβ epitope involving the free N-terminus.

D23 bound three C-terminally biotinylated variants (Aβ1–28, Aβ1–40 and Aβ1–42) with similar affinities, but did not recognize N-terminally biotinylated Aβ1–42 in ELISA (data not shown). We utilized the three monoclonal antibodies 6E10 (recognizing the N-terminus), 4G8 (central domain) and 22C4 (C-terminus) with known epitopes on the Aβ peptide to analyze the DARPin-specific epitope by competition experiments(26, 27). The addition of these antibodies to immobilized DARPin-Aβ complexes revealed that the DARPin-Aβ interaction strongly interfered with peptide recognition by antibody 6E10 and to a lesser extent by 4G8, suggesting that the N-terminal Aβ stretch was already bound by DARPin D23 (**Figure 2a**). The use of truncated Aβ1-28 during ribosome display selections focused selection on the N-terminal region. Thus, DARPin D23 does not interfere with the C-terminal antibody 22C4.

To dissect the DARPin-Aβ interaction more closely, a peptide scanning approach with soluble short Aβ fragments was used to compete the DARPin-Aβ1–28 interaction (**Figure 2b**). A 50-fold molar excess of partially overlapping peptide fragments was used for competition and only signals below those of scrambled Aβ1-42 were regarded as specific inhibition. Not only was the importance of the N-terminal aspartate residue confirmed for high-affinity binding, but we also observed that longer peptide fragments (Aβ1–16, Aβ1–38) with a free N-terminus inhibited the interaction more effectively than shorter ones, suggesting that the N-terminal stretch is part of a conformational, rather than a linear epitope. In an immunohistochemical analysis of brain sections from APP transgenic mice, we observed the specific staining of parenchymal and vascular amyloid deposits through D23 but not by the unselected control DARPin E2_5 (**Figure 2c**). Importantly, D23 does not cross-react with other brain structures in wild-type (WT) mice.

### D23 prevents Aβ1–42 aggregation and –mediated neurotoxicity.

To study the DARPin's functional effect on Aβ aggregation, equimolar concentrations of Aβ1–42 were incubated under constant agitation either alone or with DARPins D23 and the control DARPin E2_5, and thioflavin T (ThT) fluorescence signals were recorded over time (**Figure 3a**). While a 5 μM preparation of monomeric Aβ1–42 readily aggregated into fibrils, the addition of equimolar amounts of

D23 – but not E2_5 – was able to significantly prolong the lag time and reduce the elongation rate of Aβ oligomers thereby delaying the formation of higher molecular weight aggregation products. The addition of D23 to the aggregation assay resulted in a 7-fold prolonged elongation rate (elongation rates 8.58 ± 0.13 $min^{-1}$ (Aβ only), 6.28 ± 0.09 $min^{-1}$ (Aβ+E2_5) and 1.17 ± 0.01 $min^{-1}$ (Aβ+D23), whereas E2_5 only had a minor effect on the formation of Aβ fibrils. We hypothesize that D23 stabilizes the monomeric form of Aβ peptide and sequesters it from the dynamic aggregation equilibrium. This idea is underscored by the observation that D23 does not interfere with the Aβ aggregation process if added during the log-phase or after the plateau has been reached, but delays the aggregation process if added in substoichiometric amounts at the beginning of the assay (**Figure 3b**).

Aβ-mediated neurotoxicity, as measured by the release of cytoplasmic proteases from rat primary cortical neurons, was quantified either alone or in equimolar combination of Aβ with DARPin D23 or the control DARPin E2_5. The anti-Aβ DARPin could reduce toxicity by about 40%, while E2_5 did not show any effect on neurotoxicity (**Figure 3d**). We previously determined a 48 h incubation of 5 μM Aβ as most toxic to a culture of primary neurons, while an equimolar preparation of scrambled Aβ1–42 did not induce any toxicity. In microscopy experiments, we observed that the addition of D23 had a pronounced effect not only on the size of the Aβ aggregates, but also prevented dendrite retraction thereby contributing to a preserved neuronal morphology (**Figure 3c**).

**Multivalent DARPins show higher avidity on immobilized Aβ1–42.**

To further optimize Aβ binding, we constructed multivalent DARPins that were connected by flexible amino acid linkers. All constructs eluted as stable monomers from a size exclusion column with apparent molecular weights of 12 kDa (D23), 30 kDa (2xD23) and 44 kDa (3xD23) (**Figure 4a**). In ELISAs with coated Aβ1–28, the concentration of half-maximal signal ($EC_{50}$ values) of the multivalent DARPins was only slightly improved over the monomeric DARPin, consistent with only a partial multivalent engagement, presumably because head-to-tail fusions interfere with the unidirectionate display of surface-immobilized Aβ1–28 (data not shown).

An analysis of the association and dissociation phases via surface plasmon resonance (SPR) revealed substantial differences in the association and dissociation phases of the individual constructs (**Figure 4b and d**). While the monovalent DARPin D23 (**Figure 4b**) showed very fast equilibration precluding a kinetic evaluation, the trivalent construct gave rise to slower and multiphasic dissociation kinetics, indicating multivalent binding to the immobilized Aβ1–42 on the sensor chip. The monovalent construct was evaluated by measuring the plateau levels, indicating a $K_D$ of 1.589 x $10^{-7}$ M (**Figure 4c**). Since the observed association phase is the sum of the association and the dissociation process, they appear slower for the trivalent construct, simply because $k_{off}$ gets slower. Due to the various modes of multivalent binding, the sensorgrams of 3xD23 cannot be satisfactorily fit and thus no kinetic constants are reported (**Figure 4d**).

Encouraged by the long-term stability and preservation of Aβ binding activity of D23 under physiological conditions of at least three weeks (data not shown), in accordance with previous descriptions(15), we tested the effect of intracerebroventricular infusions of mono- and trivalent DARPin constructs in Tg2576 mice, which express the human APP695 isoform with the double mutation K670N/M671L(24).

**Intracerebroventricular DARPin infusion improves cognition and lowers the soluble Aβ pool in a mouse model of brain amyloidosis.**

Two weeks after intracerebroventricular implantation of osmotic pumps, all Tg2576 mice underwent Y-maze behavioral-testing, a paradigm for testing working memory in APP transgenic mice(28, 29). Cognitive assessment in the Y-maze revealed a significant improvement in percentage alternation, as a measure for memory function upon treatment with both mono- and trivalent anti-Aβ DARPins, as compared to E2_5 and PBS treated control mice ($p<0.05$, **Figure 5a**). The

number of total arm entries and distance travelled did not differ between groups (data not shown), excluding a confounding effect due to altered activity of the mice. No differences in general health measures or any treatment-induced side effects were observed across all experimental groups.

After four weeks of infusion, animals were perfused and compact plaque load in the cortex was quantified by Thioflavin S histochemical analysis of brain sections. Already after four weeks of treatment a reduction of plaque area by 23% in both D23 and 3xD23 mice was revealed, as compared to E2_5 and PBS-treated mice, but did not reach statistical significance (**Figure 5b**). As a next step, we determined Aβ levels biochemically in two sequentially extracted protein fractions from hemi brain tissue (**Figure 5c-h**). In agreement with our histological findings, D23 and 3xD23-treated mice showed a significant reduction of Aβ1–40 (by 21% and 16%), of Aβ1–38 (by 21% and 16%) and of Aβ1–42 (by 31% and 25%), respectively, in the detergent-soluble (RIPA-soluble, **Figure 5c-e**) protein fraction, as compared to E2_5 and PBS control mice. A similar trend was observed in the detergent-insoluble (formic acid soluble, **Figure 5f-h**) Aβ pool, though the effect was not significant due to the initiation phase of amyloid deposition and concomitantly higher variability of plaque load in these animals. These findings provide the first *in vivo* evidence that DARPins may successfully reverse Aβ-mediated cognitive deficits in a transgenic mouse model of brain amyloidosis and that the continuous infusion of DARPins can have a modulatory effect on brain Aβ levels.

**Discussion**

Ribosome display of combinatorial DARPin libraries has been utilized to select for DARPin binders against a diverse set of folded target proteins(10), but selection against peptide antigens without defined structure has not been reported. In this study we were able to select a DARPin binder, termed D23, which showed nanomolar affinities for the Aβ peptide in both direct and competition ELISA assays. Therefore, D23 was selected as the lead candidate for further characterization and to test the therapeutic potential of DARPins administered *in vivo* for the treatment of brain amyloidosis in APP transgenic mice.

The binding of D23 to surface-immobilized Aβ1–28 and Aβ1–42 was shown to be in the low nanomolar range; however the physiologically more relevant specific binding to Aβ in solution (as it principally occurs in prodromal phases of AD *in vivo*) is difficult to address and needed to be clarified. Aβ can occur in solution in various quaternary structures, ranging from soluble monomers(30), oligomeric intermediates(31) to fibrillar states(32). Since these forms differ in conformation, accessibility of epitopes and the possibility of bi- or even multivalent interactions, it is not surprising that Aβ-binding macromolecules can display varying specificities for Aβ, depending on its state.

A competition assay using freshly dissolved monomeric Aβ1–42 as competitor confirmed the observations made with surface-immobilized Aβ and suggested a $K_I$ value of approximately 50 nM. This inhibition was specific and not due to general hydrophobic interactions, as the use of scrambled Aβ1–42 did not significantly reduce D23 binding to the surface-immobilized target (**Figure 2b**). We had noticed that C-terminal amino acid extensions (to result in a peptide longer than the 28 residues used for selection) resulted in slightly decreased apparent affinities, possibly, because some molecules had formed aggregates and were not able to bind.

We demonstrated that the free N-terminus of the peptide must be involved in D23 binding. Furthermore, we could confirm the N-terminal Aβ domain to be involved in DARPin recognition, as of several monoclonal antibodies with comparable affinities tested(33), 6E10 was most impaired in binding the complex of D23 and Aβ1–42 and thus competes for the epitope. A peptide scanning approach enlarged this binding region to the central Aβ domain, suggesting the binding of a discontinuous rather than linear epitope, as generally described for DARPins binding to different targets(10, 12, 34). Aβ is thought to contain a largely unstructured N-terminus (residues 1–11) and two domains spanning residues 12–21 and 24–42, respectively, with varying contacts among each other, whereas the connecting residues (22 and 23) face the solvent(35). The particular binding mode of D23 is thus different from that of previously reported monoclonal antibodies that recognize a linear stretch of the Aβ peptide and also cross-react to APP(36) (at least 6E10 and 4G8).

The targeting of conformational Aβ epitopes is highly advantageous for the specificity of anti-Aβ therapeutics. As the conformation of the free monomeric Aβ peptide is most likely different from the one inside APP, D23 cross-reactivity to APP is limited (as indeed observed in cell-culture binding experiments, data not shown) and could enable repeated dosing without the risk of peripheral or central APP to either act as off-target scavenger or to create an immune reaction against APP-carrying cells. To determine the binding characteristics of D23 *ex vivo*, we performed immunohistochemical analyses with GFP-fused DARPins on brain tissue from an ArcAβ mouse model of AD (**Figure 2c**). The staining of Aβ deposits in this model with an increased proportion of vascular amyloid demonstrated D23 to preferentially bind the cross-β pleated dense central cores of the amyloid deposits, in contrast to more diffuse anti-Aβ antibody stainings. Such findings underscore D23's recognition of discontinuous amino acid stretches on both the N-terminal and central domain of the Aβ peptide that still exist in both the monomeric and aggregated form. Non-specific adherence of the DARPin scaffold to the 'sticky' amyloid plaques could be excluded, as no tissue reactivity was observed with the non-specific E2_5 control DARPin.

As a first test of the DARPin's *in vitro* activity, we were able to demonstrate that D23 delays Aβ aggregation (**Figure 3a**), using ThT

aggregation assays. In contrast, the addition of D23 during the lag phase or after complete fibrillization did not lead to any decrease in ThT signal. This likely indicates that D23 binds to and stabilizes a monomeric form of Aβ and excludes it from the aggregation process. We were further able to demonstrate that D23, but not the control DARPin E2_5, when administered into the medium of rat primary cortical neuron cultures, could reduce Aβ-mediated neurotoxicity and preserve neuronal morphology (**Figure 3b,c**).

To optimize D23 binding behavior for potential therapeutic use, a trivalent DARPin was engineered by fusing three monovalent units of D23 into one continuous open reading frame. While these constructs showed similar stability and resistance against degradation and bound the Aβ peptide with nanomolar affinity, surface plasmon resonance kinetic analysis revealed differences in on- and off-rates for each individual construct (**Figure 4b-d**). The increased molecular weight of multivalent DARPins reduces diffusion and potentially limits their tissue penetration, whereas their multivalency prolongs the half-life of DARPin-Aβ complexes in case of polymeric Aβ surfaces such as oligomers and fibrils.

Finally, we were able to demonstrate the *in vivo* therapeutic potential of D23 and 3xD23 in Tg2576 mice. Following the intracerebroventricular infusion of mono- and trivalent DARPin constructs over a 28-day-treatment, D23- and 3xD23-treated mice showed improved cognitive performance, compared to mice treated with the control DARPin E2_5 or PBS. These results were supported by histochemical analyses, showing a trend for reduction of plaque deposition in both D23- and 3xD23-treated mice (**Figure 5b**). However, as we infused anti-Aβ DARPins in Tg2576 mice already at 11 months of age, the majority of the amyloid burden is still present in soluble Aβ forms, explaining the limited number of amyloid deposits found in the cortices of treated animals.

This preventive treatment paradigm was accompanied by a biochemical analysis that showed significant reductions of brain Aβ levels for both D23- and 3xD23-treated mice with the most pronounced modulatory effects on the soluble Aβ pool (**Figure 5c-e**). Interestingly, despite anti-Aβ multivalency, 3xD23 did not perform better than its monovalent counterpart D23 *in vivo*. There are several possible explanations for this finding. If the action of D23 predominantly involves binding of monomeric Aβ, then a trimer would have, at most, the same activity as three monomers, but avidity would play no role. It is also possible that the increased molecular weight of 3xD23 could have restricted its rapid tissue penetration such that it could not sufficiently benefit from the additional interaction surfaces(15, 37).

DARPins lack the Fc domain intrinsic to the immunoglobulin G molecule, which has been shown to activate resident microglia in the vicinity of antibody-decorated amyloid deposits(29, 38, 39). Activated microglia can degrade fibrillar Aβ by lysosomal proteolysis, but local inflammatory reactions might, at worst, result in microhemorrhages (29, 40, 41). The biological activity of DARPins could be based on their association with these deposits, and they could sterically block recruitment of Aβ monomers to the amyloid plaque by binding to monomers or they could clear amyloid deposits independent of microglia in analogy to other molecular scaffolds without functional Fc domain(42–44). DARPin-mediated Aβ removal would have to rely on the capture and elimination of these species from the central nervous system via the bulk flow of interstitial fluid(45).

Our findings demonstrate the therapeutic potential of Aβ-specific DARPins for the treatment of Alzheimer's disease. With the advent of recombinant protein expression and efficient *in vitro* selection technologies, this novel class of engineered protein scaffolds presents attractive opportunities for both diagnostic and therapeutic use. If longer serum half-lives are required, this could be achieved by site-specific PEGylation(15) or by hijacking an abundant serum protein with long half-life, like albumin or immunoglobulin G through peptide tags that bind to them to escape glomerular filtration(46, 47). Knowing the recent set-backs of human anti-Aβ therapies, this study opens new avenues away from antibodies towards DARPins to fight brain amyloidosis effectively.

**Acknowledgements**
We thank K. Wollenick, W. Buck, N. Lucke and A. Jeske for excellent technical support. This study was supported in parts by the Swiss National Science Foundation and the Forschungskredit grant of the University of Zurich.

## References


1. Selkoe, D. J. (2011) Resolving controversies on the path to Alzheimer's therapeutics. *Nat. Med.* **17**, 1060–1065

2. Citron, M. (2010) Alzheimer's disease: strategies for disease modification. *Nat Rev Drug Discov* **9**, 387–398

3. Karran, E., Mercken, M., and Strooper, B. D. (2011) The amyloid cascade hypothesis for Alzheimer's disease: an appraisal for the development of therapeutics. *Nat. Rev. Drug. Discov.* **10**, 698–712

4. Schenk, D., Barbour, R., Dunn, W., Gordon, G., Grajeda, H., Guido, T., Hu, K., Huang, J., Johnson-Wood, K., Khan, K., Kholodenko, D., Lee, M., Liao, Z., Lieberburg, I., Motter, R., Mutter, L., Soriano, F., Shopp, G., Vasquez, N., Vandevert, C., Walker, S., Wogulis, M., Yednock, T., Games, D., and Seubert, P. (1999) Immunization with amyloid-beta attenuates Alzheimer-disease-like pathology in the PDAPP mouse. *Nature* **400**, 173–177

5. Morgan, D., Diamond, D. M., Gottschall, P. E., Ugen, K. E., Dickey, C., Hardy, J., Duff, K., Jantzen, P., DiCarlo, G., Wilcock, D., Connor, K., Hatcher, J., Hope, C., Gordon, M., and Arendash, G. W. (2000) Abeta peptide vaccination prevents memory loss in an animal model of Alzheimer's disease. *Nature* **408**, 982–985

6. Rinne, J. O., Brooks, D. J., Rossor, M. N., Fox, N. C., Bullock, R., Klunk, W. E., Mathis, C. A., Blennow, K., Barakos, J., Okello, A. A., de LIano, S. R. M., Liu, E., Koller, M., Gregg, K. M., Schenk, D., Black, R., and Grundman, M. (2010) 11C-PiB PET assessment of change in fibrillar amyloid-beta load in patients with Alzheimer's disease treated with bapineuzumab: a phase 2, double-blind, placebo-controlled, ascending-dose study. *Lancet Neurol.* **9**, 363–372

7. Siemers, E. R., Friedrich, S., Dean, R. A., Gonzales, C. R., Farlow, M. R., Paul, S. M., and Demattos, R. B. (2010) Safety and changes in plasma and cerebrospinal fluid amyloid beta after a single administration of an amyloid beta monoclonal antibody in subjects with Alzheimer disease. *Clin. Neuropharmacol.* **33**, 67–73

8. Relkin, N. R., Szabo, P., Adamiak, B., Burgut, T., Monthe, C., Lent, R. W., Younkin, S., Younkin, L., Schiff, R., and Weksler, M. E. (2009) 18-Month study of intravenous immunoglobulin for treatment of mild Alzheimer disease. *Neurobiol. Aging* **30**, 1728–1736

9. Delrieu, J., Ousset, P. J., Caillaud, C., and Vellas, B. (2012) "Clinical trials in Alzheimer"s disease': immunotherapy approaches. *J. Neurochem.* **120**, 186–193

10. Boersma, Y. L., and Plückthun, A. (2011) DARPins and other repeat protein scaffolds: advances in engineering and applications. *Curr. Opin. Biotechnol.* **22**, 849–857

11. Binz, H. K., Stumpp, M. T., Forrer, P., Amstutz, P., and Plückthun, A. (2003) Designing repeat proteins: well-expressed, soluble and stable proteins from combinatorial libraries of consensus ankyrin repeat proteins. *J. Mol. Biol* **332**, 489–503

12. Binz, H. K., Amstutz, P., Kohl, A., Stumpp, M. T., Briand, C., Forrer, P., Grütter, M. G., and Plückthun, A. (2004) High-affinity binders selected from designed ankyrin repeat protein libraries. *Nat. Biotechnol* **22**, 575–582

13. Amstutz, P., Binz, H. K., Parizek, P., Stumpp, M. T., Kohl, A., Grütter, M. G., Forrer, P., and Plückthun, A. (2005) Intracellular kinase inhibitors selected from combinatorial libraries of designed ankyrin repeat proteins. *J. Biol. Chem.* **280**, 24715–24722

14. Kohl, A., Amstutz, P., Parizek, P., Binz, H. K., Briand, C., Capitani, G., Forrer, P., Plückthun, A., and Grütter, M. G. (2005) Allosteric inhibition of aminoglycoside phosphotransferase by a designed ankyrin repeat protein. *Structure* **13**, 1131–1141

15. Zahnd, C., Kawe, M., Stumpp, M. T., de Pasquale, C., Tamaskovic, R., Nagy-Davidescu, G., Dreier, B., Schibli, R., Binz, H. K., Waibel, R., and Plückthun, A. (2010) Efficient tumor targeting with high-affinity designed ankyrin repeat proteins: effects of affinity and molecular size. *Cancer Res* **70**, 1595–1605

16. Banks, W. A., Terrell, B., Farr, S. A., Robinson, S. M., Nonaka, N., and Morley, J. E. (2002) Passage of amyloid beta protein antibody across the blood-brain barrier in a mouse model of Alzheimer's disease. *Peptides* **23**, 2223–2226

17. Bard, F., Cannon, C., Barbour, R., Burke, R. L., Games, D., Grajeda, H., Guido, T., Hu, K., Huang, J., Johnson-Wood, K., Khan, K., Kholodenko, D., Lee, M., Lieberburg, I., Motter, R., Nguyen, M., Soriano, F., Vasquez, N., Weiss, K., Welch, B., Seubert, P., Schenk, D., and Yednock, T. (2000) Peripherally administered antibodies against amyloid beta-peptide enter the central nervous system and reduce pathology in a mouse model of Alzheimer disease. *Nat. Med* **6**, 916–919

18. Levites, Y., Smithson, L. A., Price, R. W., Dakin, R. S., Yuan, B., Sierks, M. R., Kim, J., McGowan, E., Reed, D. K., Rosenberry, T. L., Das, P., and Golde, T. E. (2006) Insights into the mechanisms of action of anti-Abeta antibodies in Alzheimer's disease mouse models. *FASEB J* **20**, 2576–2578

19. Stumpp, M. T., Binz, H. K., and Amstutz, P. (2008) DARPins: a new generation of protein therapeutics. *Drug Discov. Today* **13**, 695–701

20. Cattepoel, S., Hanenberg, M., Kulic, L., and Nitsch, R. M. (2011) Chronic Intranasal Treatment with an Anti-Aβ30-42 scFv Antibody Ameliorates Amyloid Pathology in a Transgenic Mouse Model of Alzheimer's Disease. *PLoS ONE* **6**, e18296

21. Zahnd, C., Amstutz, P., and Plückthun, A. (2007) Ribosome display: selecting and evolving proteins in vitro that specifically bind to a target. *Nat. Methods* **4**, 269–279

22. Wetzel, S. K., Settanni, G., Kenig, M., Binz, H. K., and Plückthun, A. (2008) Folding and Unfolding Mechanism of Highly Stable Full-Consensus Ankyrin Repeat Proteins. *Journal of Molecular Biology* **376**, 241–257

23. Finder, V. H., Vodopivec, I., Nitsch, R. M., and Glockshuber, R. (2010) The Recombinant Amyloid-beta Peptide Abeta 1-42 Aggregates Faster and Is More Neurotoxic than Synthetic Abeta 1-42. *J Mol Biol* **396**, 9–18

24. Hsiao, K., Chapman, P., Nilsen, S., Eckman, C., Harigaya, Y., Younkin, S., Yang, F., and Cole, G. (1996) Correlative Memory Deficits, Aβ Elevation, and Amyloid Plaques in Transgenic Mice. *Science* **274**, 99 –103

25. Biscaro, B., Lindvall, O., Hock, C., Ekdahl, C. T., and Nitsch, R. M. (2009) Abeta immunotherapy protects morphology and survival of adult-born neurons in doubly transgenic APP/PS1 mice. *J. Neurosci* **29**, 14108–14119

26. Kim et al. (1988) Production and characterization of monoclonal antibodies reactive to synthetic cerebrovascular amyloid peptide. *Neurosci. Res. Commun.* **2**, 121–130

27. Mohajeri, M. H., Saini, K., Schultz, J. G., Wollmer, M. A., Hock, C., and Nitsch, R. M. (2002) Passive immunization against β-amyloid peptide protects central nervous system (CNS) neurons from increased vulnerability associated with an Alzheimer's disease-causing mutation. *J. Biol. Chem.* **277**, 33012 –33017

28. Arendash, G. W., Gordon, M. N., Diamond, D. M., Austin, L. A., Hatcher, J. M., Jantzen, P., DiCarlo, G., Wilcock, D., and Morgan, D. (2001) Behavioral assessment of Alzheimer's transgenic mice following long-term Abeta vaccination: task specificity and correlations between Abeta deposition and spatial memory. *DNA Cell Biol.* **20**, 737–744

29. Wilcock, D. M., Rojiani, A., Rosenthal, A., Levkowitz, G., Subbarao, S., Alamed, J., Wilson, D., Wilson, N., Freeman, M. J., Gordon, M. N., and Morgan, D. (2004) Passive amyloid immunotherapy clears amyloid and transiently activates microglia in a transgenic mouse model of amyloid deposition. *J. Neurosci.* **24**, 6144–6151

30. DeMattos, R. B., Bales, K. R., Cummins, D. J., Dodart, J.-C., Paul, S. M., and Holtzman, D. M. (2001) Peripheral anti-Aβ antibody alters CNS and plasma Aβ clearance and decreases brain Aβ burden in a mouse model of Alzheimer's disease. *Proc Natl Acad Sci USA* **98**, 8850 –8855

31. Kayed, R., Head, E., Thompson, J. L., McIntire, T. M., Milton, S. C., Cotman, C. W., and Glabe, C. G. (2003) Common Structure of Soluble Amyloid Oligomers Implies Common Mechanism of Pathogenesis. *Science* **300**, 486 –489

32. O'Nuallain, B., and Wetzel, R. (2002) Conformational Abs recognizing a generic amyloid fibril epitope. *Proc. Natl. Acad. Sci. USA.* **99**, 1485–1490

33. Ramakrishnan, M., Kandimalla, K. K., Wengenack, T. M., Howell, K. G., and Poduslo, J. F. (2009) Surface Plasmon Resonance Binding Kinetics of Alzheimer's Disease Amyloid β Peptide-Capturing and Plaque-Binding Monoclonal Antibodies. *Biochemistry* **48**, 10405–10415

34. Schweizer, A., Roschitzki-Voser, H., Amstutz, P., Briand, C., Gulotti-Georgieva, M., Prenosil, E., Binz, H. K., Capitani, G., Baici, A., Plückthun, A., and Grütter, M. G. (2007) Inhibition of caspase-2 by a designed ankyrin repeat protein: specificity, structure, and inhibition mechanism. *Structure* **15**, 625–636

35. Vitalis, A., and Caflisch, A. (2010) Micelle-like architecture of the monomer ensemble of Alzheimer's amyloid-β peptide in aqueous solution and its implications for Aβ aggregation. *J. Mol. Biol* **403**, 148–165

36. Tampellini, D., Magrané, J., Takahashi, R. H., Li, F., Lin, M. T., Almeida, C. G., and Gouras, G. K. (2007) Internalized Antibodies to the Aβ Domain of APP Reduce Neuronal Aβ and Protect against Synaptic Alterations. *J. Biol. Chem.* **282**, 18895 –18906

37. Colcher, D., Pavlinkova, G., Beresford, G., Booth, B. J., Choudhury, A., and Batra, S. K. (1998) Pharmacokinetics and biodistribution of genetically-engineered antibodies. *Q J Nucl Med* **42**, 225–241

38. Koenigsknecht-Talboo, J., Meyer-Luehmann, M., Parsadanian, M., Garcia-Alloza, M., Finn, M. B., Hyman, B. T., Bacskai, B. J., and Holtzman, D. M. (2008) Rapid microglial response around amyloid pathology after systemic anti-Abeta antibody administration in PDAPP mice. *J. Neurosci* **28**, 14156–14164

39. Wang, A., Das, P., Switzer, R. C., 3rd, Golde, T. E., and Jankowsky, J. L. (2011) Robust amyloid clearance in a mouse model of Alzheimer's disease provides novel insights into the mechanism of amyloid-beta immunotherapy. *J. Neurosci* **31**, 4124–4136

40. Racke, M. M., Boone, L. I., Hepburn, D. L., Parsadainian, M., Bryan, M. T., Ness, D. K., Piroozi, K. S., Jordan, W. H., Brown, D. D., Hoffman, W. P., Holtzman, D. M., Bales, K. R., Gitter, B. D., May, P. C., Paul, S. M., and DeMattos, R. B. (2005) Exacerbation of cerebral amyloid angiopathy-associated microhemorrhage in amyloid precursor protein transgenic mice by immunotherapy is dependent on antibody recognition of deposited forms of amyloid beta. *J. Neurosci.* **25**, 629–636

41. Pfeifer, M., Boncristiano, S., Bondolfi, L., Stalder, A., Deller, T., Staufenbiel, M., Mathews, P. M., and Jucker, M. (2002) Cerebral hemorrhage after passive anti-Abeta immunotherapy. *Science* **298**, 1379

42. Bacskai, B. J., Kajdasz, S. T., McLellan, M. E., Games, D., Seubert, P., Schenk, D., and Hyman, B. T. (2002) Non-Fc-mediated mechanisms are involved in clearance of amyloid-beta in vivo by immunotherapy. *J. Neurosci* **22**, 7873–7878

43. Wilcock, D. M., DiCarlo, G., Henderson, D., Jackson, J., Clarke, K., Ugen, K. E., Gordon, M. N., and Morgan, D. (2003) Intracranially administered anti-Abeta antibodies reduce beta-amyloid deposition by mechanisms both independent of and associated with microglial activation. *J. Neurosci* **23**, 3745–3751

44. Wilcock, D. M., Alamed, J., Gottschall, P. E., Grimm, J., Rosenthal, A., Pons, J., Ronan, V., Symmonds, K., Gordon, M. N., and Morgan, D. (2006) Deglycosylated anti-amyloid-beta antibodies eliminate cognitive deficits and reduce parenchymal amyloid with minimal vascular consequences in aged amyloid precursor protein transgenic mice. *J. Neurosci* **26**, 5340–5346

45. Shibata, M., Yamada, S., Kumar, S. R., Calero, M., Bading, J., Frangione, B., Holtzman, D. M., Miller, C. A., Strickland, D. K., Ghiso, J., and Zlokovic, B. V. (2000) Clearance of Alzheimer's amyloid-β1-40 peptide from brain by LDL receptor–related protein-1 at the blood-brain barrier. *J. Clin. Invest.* **106**, 1489–1499

46. Dennis, M. S., Zhang, M., Meng, Y. G., Kadkhodayan, M., Kirchhofer, D., Combs, D., and Damico, L. A. (2002) Albumin binding as a general strategy for improving the pharmacokinetics of proteins. *J. Biol. Chem* **277**, 35035–35043

47. Nguyen, A., Reyes, A. E., Zhang, M., McDonald, P., Wong, W. L. T., Damico, L. A., and Dennis, M. S. (2006) The pharmacokinetics of an albumin-binding Fab (AB.Fab) can be modulated as a function of affinity for albumin. *Protein Eng. Des. Sel.* **19**, 291–297

**Figure legends**

**Figure 1** Selection of anti-Aβ DARPins through ribosome display *in vitro*. **(a)** DARPin libraries were selected against decreasing amounts of the biotinylated Aβ1-28 peptide via ribosome display in four selection rounds. Biotinylated peptides were presented via neutravidin immobilized on a microtiter plate (round 1) or recovered from solution through streptavidin-coated magnetic particles in all subsequent rounds. DNA was re-amplified at the end of each round with decreasing numbers of PCR cycles (arrow numbers). After four rounds, *E. coli* was transformed, and individual clones were analyzed for Aβ binding activity through ELISA. **(b)** ELISA titration with increasing amounts of DARPin D23 binding to immobilized Aβ1-28 and Aβ1-42. The half maximal intensity ($EC_{50}$) is determined at 17 nM (Aβ1-28) and 31 nM (Aβ1-42). A non-selected library member, E2_5, did not bind Aβ1-42 at any concentration. **(c)** Inhibition of DARPin D23 binding to immobilized Aβ1-28-biotin by increasing concentrations of the soluble non-biotinylated peptide Aβ1-42. The competition showed half-maximal inhibition at approximately 50 nM Aβ1-42. Data in **b-c** are means from three independent experiments; represented as means ± SD.

**Figure 2** Determination of the DARPin D23 epitope and binding to amyloid deposits in *ex vivo* murine brain tissue. **(a)** In a direct ELISA, Aβ1-42 was bound to immobilized DARPin D23, and the accessibility of different parts of the peptide was probed with monoclonal anti-Aβ antibodies directed against the N-terminus (6E10), central part (4G8) or C-terminus (22c4) of the peptide. The lowest binding signal was observed for antibody 6E10, specific for the N-terminus of Aβ. **(b)** Determination of the Aβ epitope recognized by D23 by competition with a 50-fold molar excess of Aβ-derived peptide fragments. Biotinylated Aβ1-28 peptide was immobilized via streptavidin and ELISA signals were normalized to a non-competed control. Inhibition was considered specific if signals were below the one of scrambled Aβ1-42 control (dotted line). **(c)** GFP-fused DARPin D23 specifically recognized amyloid-β plaques in brain slices from transgenic ArcAβ mice. The specificity of plaque binding by the selected DARPin D23 was confirmed by applying DARPins C-terminally fused to superfolder GFP (sfGFP) onto brain sections from wild-type mice (A-C) and ArcAβ (D-F) transgenic mice. The control DARPin E2_5 did not show any binding activity (G-H). D23 recognized vascular (arrow) and parenchymal (arrowhead) amyloid deposits without cross-reactivity to WT brain structures. First row: DARPin binding (GFP channel); middle row: anti-Aβ antibody binding (antibody 4G8, Cy3 channel); bottom row: merge of GFP- and Cy3-channel. Data in **a-b** are means from three independent experiments; represented as means ± SD.

**Figure 3** Inhibition of Aβ aggregation and Aβ-mediated neurotoxicity through D23 addition. **(a)** The inhibitory effect of DARPin D23 on Aβ1-42 aggregation was monitored by thioflavin T fluorescence (ThT). Equimolar concentrations of Aβ1-42 and DARPins D23 or E2_5 (5 µM each) were co-incubated and ThT fluorescence monitored for 3 hours at 489 nm. The assays were performed in triplicates in stirred cuvettes. Data presented as means ± SD. **(b)** Half-equimolar concentrations of D23 were added at different timepoints during the exponential growth phase of the Aβ fibrils. The addition occurred at $t_1$=20 min (red curve) and $t_2$=37 min (gray curve). **(c)** Effects of Aβ1-42 and DARPin addition on neuronal morphology. Upper panels: neurons were incubated either in the absence (-) or in the presence (+) of 5 µM Aβ1-42. Aβ deposits were stained orange (polyclonal anti-Aβ antibody), neurons green (antibody to MAP2). Lower panels: co-incubation of Aβ1-42 with Aβ-specific DARPin D23 (left, lower panel) or control DARPin E2_5 (right, lower panel). Inlays to all four micrographs show magnifications of anti-MAP2 stained neurons from the aforementioned treatment conditions. Scale bars correspond to 20 µm. **(d)** Primary rat neurons (day 5 in vitro) were co-incubated with equimolar amounts of recombinant Aβ1-42 and DARPins D23 or E2_5 (all components 5 µM). After 48 hours the level of Aβ1-42-mediated toxicity was assessed by the activity of neuronal proteases (cleaving luciferin off a coupled substrate). D23 is able to significantly decrease Aβ1-42-mediated cytotoxicity as compared to controls (mean ± SEM; * $p < 0.05$; One-way ANOVA, followed by Tukey's test).

**Figure 4** Stability and binding of multivalent DARPin constructs to immobilized Aβ1-42. **(a)** Multivalent DARPin variants of D23 were constructed by fusing monovalent units by $(Gly_4Ser)_2$ linkers. These constructs were well expressed and eluted as monomeric peaks from size exclusion chromatography with apparent molecular weights of 12 kDa ($V_E$=1.86 mL, D23), 30.4 kDa ($V_E$= 1.57 mL, 2xD23) and 44.3 kDa ($V_E$=1.45 mL, 3xD23). The elution volumes of MW standards are shown above the graph. **(b)** Surface plasmon resonance (SPR) kinetics of monovalent DARPin D23 on surface-immobilized Aβ1-42. The C-terminally biotinylated peptide Aβ1-42 was immobilized on a streptavidin sensor chip and monovalent DARPin D23 was injected in duplicates at increasing concentrations of 1 to 128 nM. Association and dissociation phases were recorded and the sensorgrams were globally fitted (red dotted lines) to a 1:1 binding model. **(c)** The equilibrium binding constant ($K_D$) of monovalent D23 was determined as 1.59 x $10^{-7}$ M from evaluation of the plateau heights as function of D23 concentration. **(d)** SPR kinetics of trivalent DARPin on surface-immobilized Aβ1-42. Trivalent 3xD23 was attempted to be fitted with a bivalent binding model (red dotted lines), but the more complicated situation with several modes of bivalent and possibly trivalent binding are not described by the fits well enough and preclude a numerical evaluation.

**Figure 5** Restoration of memory deficits in APPSwe transgenic mice by DARPin treatment and influence on soluble brain Aβ levels. **(a)** Two weeks after continuous intracerebroventricular infusion of monovalent (hatched), trivalent (black) DARPins, non-specific DARPin (E2_5, grey) or PBS (white), Tg2576 mice were cognitively assessed in a Y-maze experiment by recording the number of alternating arm entries. **(b)** After four weeks of anti-Aβ therapy, animals were sacrificed and the brain cortical area covered by amyloid deposits determined. DARPin treatment appeared to influence amyloid deposition, but did not reach significance. **(c)-(h)** Total levels of both soluble (RIPA dissolved, **c-e**) and insoluble (formic acid dissolved, **f-h**) brain Aβ1-38, Aβ1-40 and Aβ1-42 levels were measured with a human Abeta triplex kit. Animals per group n = 10-12. Data shown as mean ± SEM. Statistical analysis by ANOVA followed by Mann Whitney U test; * $p<0.05$; # trend $p<0.10$.

## Figures

### Figure 1

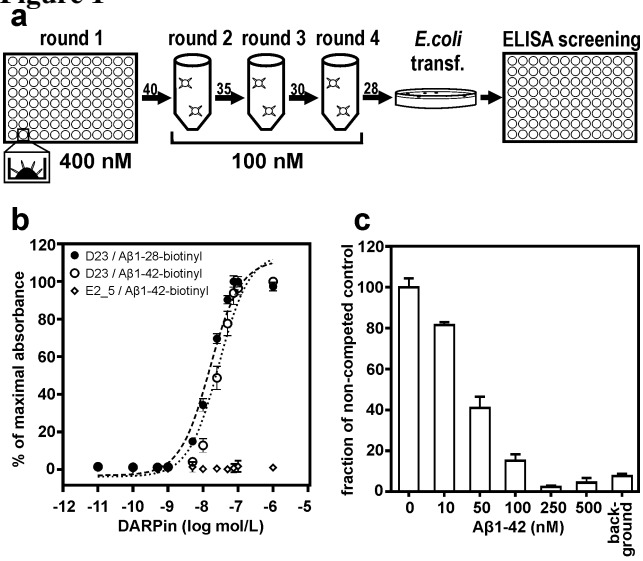


### Figure 2

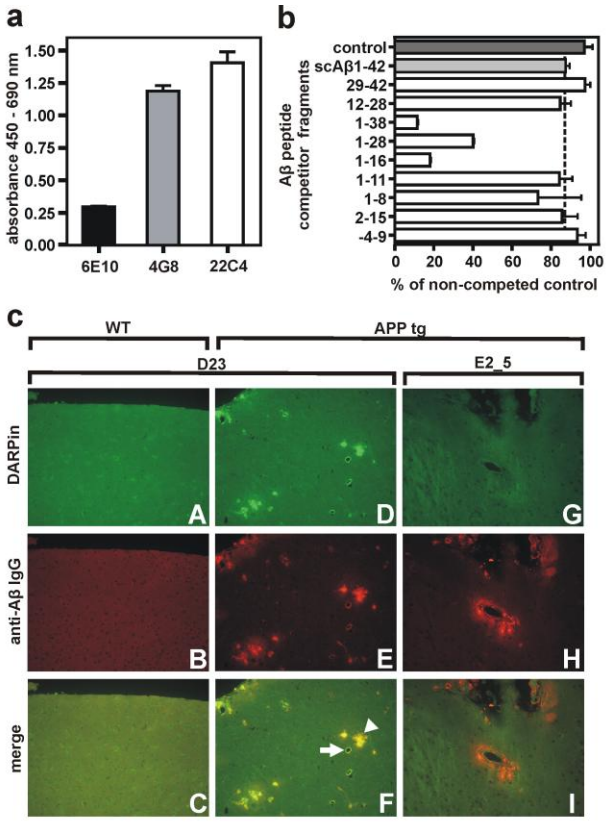

**Figure 3**

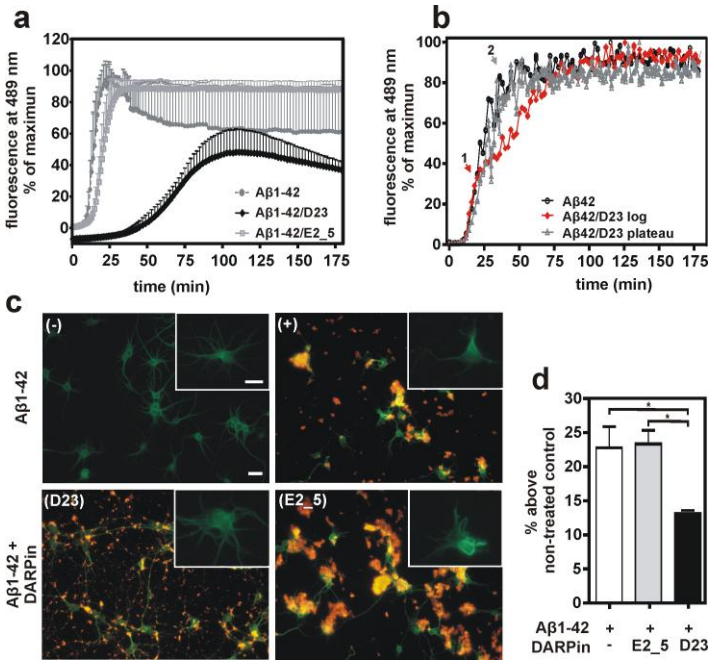


**Figure 4**

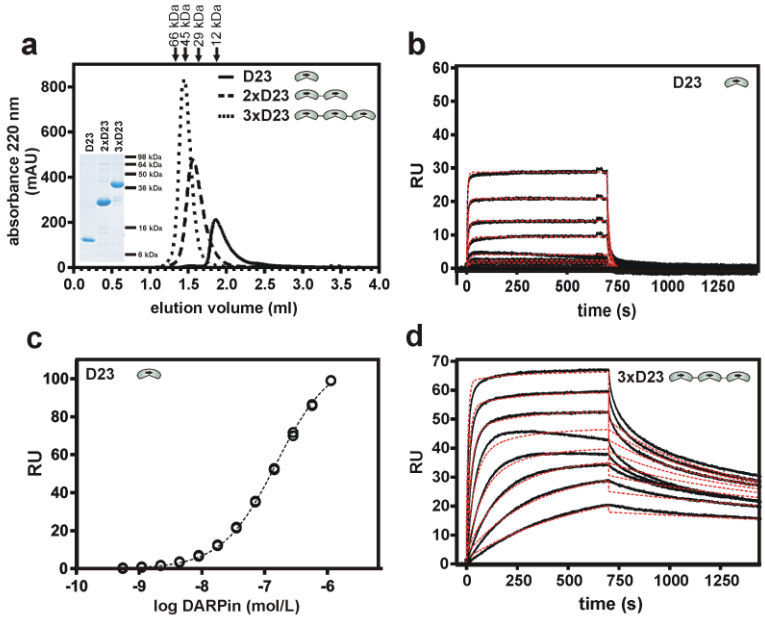

**Figure 5**

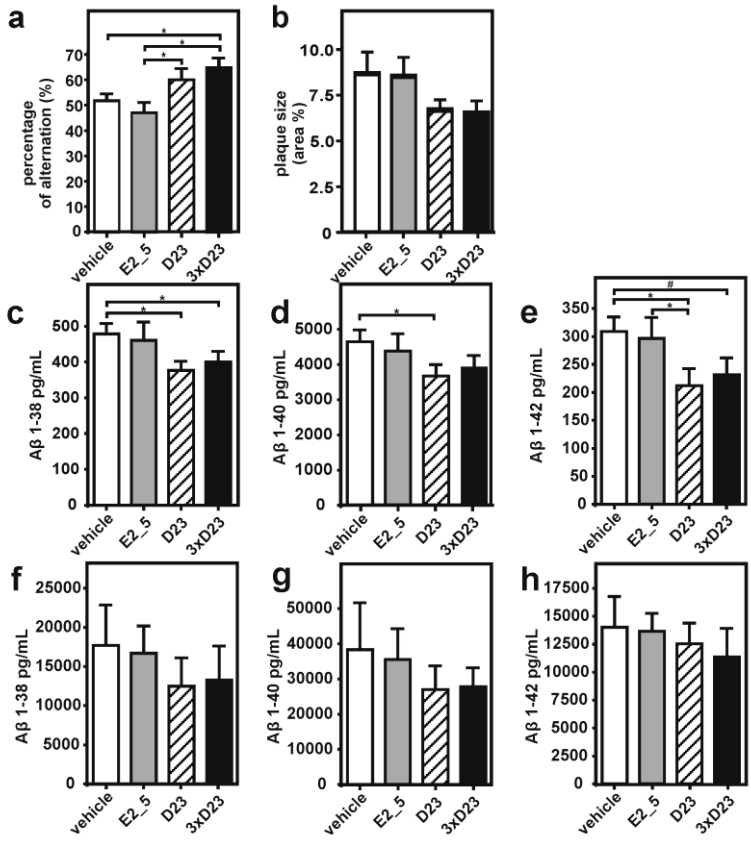


Neurobiology:

# Aβ-specific DARPins as a novel class of potential therapeutics for Alzheimer's disease


Michael Hanenberg, Jordan McAfoose, Luka Kulic, Tobias Welt, Fabian Wirth, Petra Parizek, Lisa Strobel, Susann Cattepoel, Claudia Späni, Rebecca Derungs, Marcel Maier, Andreas Plückthun and Roger M. Nitsch

*J. Biol. Chem. published online August 12, 2014*

---

Access the most updated version of this article at doi: 10.1074/jbc.M114.564013



This article cites 0 references, 0 of which can be accessed free at
http://www.jbc.org/content/early/2014/08/12/jbc.M114.564013.full.html#ref-list-1